PHYSICAL REVIEW E **79**, 010401(R) (2009)

Aggregation phenomena in telechelic star polymer solutions

Federica Lo Verso,[1,*] Athanassios Z. Panagiotopoulos,[2] and Christos N. Likos[3]
[1]*Chimie Analytique et Biophysico-chimie de l' Environnement (CABE), Université de Genève—Sciences II, 30 Quai Ernest-Ansermet, CH-1211 Genève 4, Switzerland*
[2]*Department of Chemical Engineering and PRISM, Princeton University, Princeton, New Jersey 08540, USA*
[3]*Institute for Theoretical Physics II: Soft Matter, Heinrich-Heine-Universität Düsseldorf, D-40225 Düsseldorf, Germany*
(Received 16 October 2008; published 16 January 2009)

Telechelic star polymers are macromolecules with functionalized, mutually attractive end groups. We employ computer simulations on a lattice to investigate the phase behavior of trifunctional telechelic stars as a function of the fraction λ of attractive terminal monomers. We find macrophase separation that disappears at some value $0.4<\lambda<0.5$, at which point it is replaced by self-organization into interconnected micelles. We supplement the thermodynamics with a morphometric analysis that provides insight into the mesostructure of the resulting aggregates.

DOI: 10.1103/PhysRevE.79.010401 PACS number(s): 82.70.Uv, 61.25.he, 83.80.Qr, 87.15.bk

Recent advances in the synthesis of functionalized, associating colloids have led to an outburst of activity in understanding their extremely rich self-assembly properties [1]. Currently popular systems are patchy colloids with a small number of attractive patches [2] as well as single-strand DNA-coated colloids [3,4], which have been recently shown to assemble into interpenetrating networks, featuring multiple critical points [5]. At the other end of the spectrum lie flexible block copolymers, whose association properties have been the subject of studies for a long time, including lattice simulation [6] and coarse-grained theoretical approaches [7,8]. Telechelic star polymers (TSP's) are a hybrid system that combines the flexibility of chains with the sphericity of colloids [9] and are thus promising candidates for tuning the self-assembly, the rheology, and the properties of soft matter. Composite materials that combine colloids with telechelic *chains* have been studied for the cases of colloidal nanospheres [10] and emulsions [11], whereas quite a bit of attention has been devoted, experimentally [12,13] and theoretically [14–16], to planar telechelic brushes. Little is known about bulk TSP solutions, although experimental realizations of TSP melts are readily available in the form of zwitterionic star polybutadienes [17–19]. On the basis of rheological and scattering data, a variety of self-organizing scenarios for mono-, di-, and tri-ω-functionalized, $f=3$-arm TSP's has been put forward [18,19]. For di-ω-functionalized TSP's, system-spanning networks, and tri-ω-functionalized TSP's formation of aggregates has been suggested but, in the absence of optical observation methods and of theory or simulation insights, the situation is still unclear.

The self-aggregation of a TSP in dilute solutions has been recently analyzed by analytical theory and simulations [20–22]. It was found that, at sufficiently low temperatures, low-functionality TSP's collapse from an open to a *watermelon* configuration and that intermediate-functionality TSP's feature conformations with separated globules at the arms' ends. At finite concentrations, intermolecular aggregation processes are expected to give rise to novel features. In this Rapid Communication, we report on a detailed investigation of the problem, resorting to Monte Carlo simulations of a lattice model, which greatly enhances the speed of the calculation without compromising the physical picture. We construct molecules that consist of f chains anchored on a common center; each chain contains n monomers, whereby p of them are heads (H) and q are terminal tails (T); the central monomer is always of the H type. A molecular architecture is thereby coded as $H(H_pT_q)_f$. In what follows, we consider exclusively $f=3$ and $n=10$, modifying only the number of attractive tails q or, equivalently, the fraction $\lambda=q/n$ of end monomers per chain. We demonstrate that for $q\geqslant 5$ macroscopic phase separation between a dilute and a dense phase takes place, accompanied by a percolation transition that ends at the binodal line at the low-density side of the critical point. The binodals shift to lower temperatures as λ diminishes and disappear altogether at some threshold $0.4<\lambda<0.5$, giving way to the formation of multiply connected micelles.

We employed grand canonical Monte Carlo (GCMC) simulations on a three-dimensional cubic lattice with a coordination number of 26 and periodic boundary conditions, in order to examine concentrated solutions of TSP's. In this fashion, chains have higher flexibility than would be the case for a coordination number of 6 and correspond to effectively longer arms. The relative position vectors for the interactions are (1,0,0), (1,1,0), (1, 1, 1), together with the additional vectors arising from the point-group symmetry operations of the cubic lattice [23,24]. For the interactions, we employ the Larson model [25], in which the lattice is completely occupied, either by monomers or by the solvent (S). Site-site interaction energies ϵ_{ij}, $i,j=H$, T, or S, vanish for separations beyond the coordination number of a given site. The solvent molecules S are identical to the head (inner) monomers H of the arms, reducing the number of microscopic energy parameters to three: ϵ_{HH}, ϵ_{HT}, and ϵ_{TT}. Every rearrangement entails an energy change $\epsilon=2\epsilon_{HT}-\epsilon_{HH}-\epsilon_{TT}$ [23–25]; thus ϵ sets an energy scale of the problem at hand. Without loss of generality, we choose $\epsilon=1$ and, in particular, $\epsilon_{HT}=\epsilon_{HH}=0$ and $\epsilon_{TT}=-1$. The dimensionless temperature is defined as T^*

*Present address: Institute of Physics, Johannes-Gutenberg-University of Mainz, Staudinger Weg 7, D-55099 Mainz, Germany.

$=k_BT/\epsilon$, where T is the absolute temperature and k_B stands for the Boltzmann constant.

We considered box lengths $L=20$ and 30 lattice constants. The instantaneous number of monomers in the system is denoted $\mathcal{N}$, whereas $N\equiv\langle\mathcal{N}\rangle_{\mu,V,T}$ stands for the expectation value of the same in the simulated GC ensemble with chemical potential μ and volume $V=L^3$; thereby, $\phi=N/V$ is the average monomer concentration. A mixture of displacement, single regrowth, and cluster moves was performed, to accelerate sampling, in particular for the high-concentration solutions. The cluster-move routine picks up a random TSP and moves the cluster to which it belongs by a fixed amount; here, in the cluster definition any amphiphilic monomer is counted as part of the cluster, heads as well as tails, to make the routine reasonably efficient. Insertions and removals of TSP's or individual arms of the latter were performed computing the Rosenbluth weight for each growth step [26]. A total of 10^6 to 10^9 MC steps were employed, depending on the region of the phase diagram under investigation. Data for the histograms for $\mathcal{N}$ as well as the internal energy $\mathcal{U}$ for a given system size were combined using the Ferrenberg-Swendsen algorithm [27,28] and analyzed to determine the critical point by matching the distribution of the linear combination $\mathcal{M}=\mathcal{N}-s\mathcal{U}$, with the appropriate mixing parameter s, to the universal, Ising order-parameter distribution [23,24,29,30]. The pressure P was calculated employing the methods described in [6]. The GCMC simulations predict fluid-fluid phase separation and several aggregation processes such as the formation of sponge and micellar phases, depending on the temperature, density, and fraction λ of tail monomers. The resulting variety of the phases is further characterized by our morphological analysis.

When $q\geqslant 5$, the system undergoes phase separation into a dilute and a dense phase. Different system sizes are crucial in determining whether the system undergoes a macroscopic phase transition or microphase separation. In the former case, the binodals obtained for two different sizes coincide whereas in the latter the apparent binodals for two different systems sizes differ markedly, the ones arising from the larger size being much more narrow [6]. On the contrary, the pressure curves show considerable finite-size dependence for macrophase separation and very weak one for microphase ordering. The results for the coexistence binodals are summarized in Fig. 1. The two-phase regions shift to lower temperature and the critical monomer concentration decreases as the number of attractive monomers is lowered. The ordering of the high-density phases for these systems is nontrivial. With increasing ϕ, the end monomers self-organize into bicontinuous phases at low T^*; see the inset of Fig. 1. These are multiply connected, percolating phases, lying on the gel side of the denoted sol-gel line.

Our results are qualitatively similar to those of Bianchi *et al.* [2] pertaining to patchy colloids that feature M attractive patches. Also in that case the binodals shrink as M decreases to its minimal value, $M=2$, giving rise to *empty liquids*. At variance with the case of patchy colloids, however, in our case the flexibility of the chains opens up new ways for the system to self-organize. Instead of observing an ever-shrinking density gap as $\lambda\rightarrow 0$, the TSP binodals *disappear abruptly* at some threshold value $0.4<\lambda<0.5$, where micelle formation arises. A similar transition from phase coexistence to micellization has been seen in linear diblock analogs of this model [6]. The micelles consist of a core in which the T-type, terminal monomers of g_0 chains aggregate, whereas their outer part consists of the inner, H-type monomers of the arms.

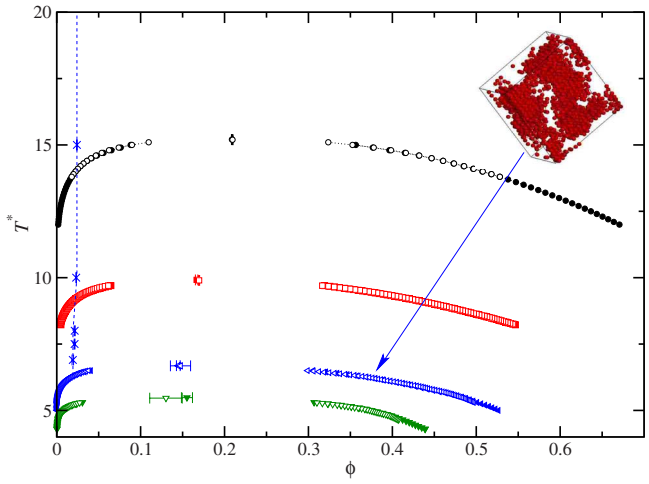

FIG. 1. (Color online) Phase coexistence curves obtained from GCMC simulations and the histogram reweighting technique for two sizes L of the simulation box. Filled symbols: $L=20$; empty symbols: $L=30$. Curves from top to bottom are for $H(H_0T_{10})_3$, $H(H_2T_8)_3$, $H(H_4T_6)_3$, and $H(H_5T_5)_3$. The dashed line denotes the percolation transition for the $H(H_4T_6)_3$ system. The inset shows a snapshot of the terminal monomers of the same system at the point indicated by the arrow.

Micellization occurs beyond the critical micelle concentration (CMC). Quantitative evidence for the formation of micelles is offered by the histograms of the number of chains, N_{ch}, participating in a micellar cluster, $P(N_{ch})$, shown as examples in Figs. 2 and 3 for $H(H_6T_4)_3$ and $H(H_8T_2)_3$, respectively. Here, a cluster is defined by all terminal monomers that are found within the distance set by the coordination of the lattice and which are rendered as red spheres in the snapshots of Figs. 2 and 3. The CMC of the $H(H_6T_4)_3$ system, determined by the change of the slope in the osmotic pressure vs ϕ curves, lies at $\phi_{CMC}=0.070\pm 0.002$, whereas that of $H(H_8T_2)_3$ is at $\phi_{CMC}=0.092\pm 0.002$. A smaller fraction of attractive tails results into a higher concentration needed for micellization but in both cases ϕ_{CMC} is low. Our findings are consistent with scattering intensities from three-ω-functionalized zwitterionic stars [18]. There, a structural peak shows up at low temperatures, which gradually disappears as T is raised, and the stickiness that leads to micelle formation is overtaken by thermal energy.

In the $P(N_{ch})$ histograms of Figs. 2 and 3, the onset of micellization is marked by the development of a shoulder in the corresponding distribution, which extends out to the aggregation number g_0 of the micelles. The latter features only a very weak dependence with ϕ for both systems shown and lies at $g_0\cong 55$ for the $H(H_6T_4)_3$ case and at $g_0\cong 45$ for the less attractive, $H(H_8T_2)_3$ one. The insensitivity of g_0 to ϕ implies that the formed micelles are already sterically saturated in their cores; thus an increase in monomer concentra-

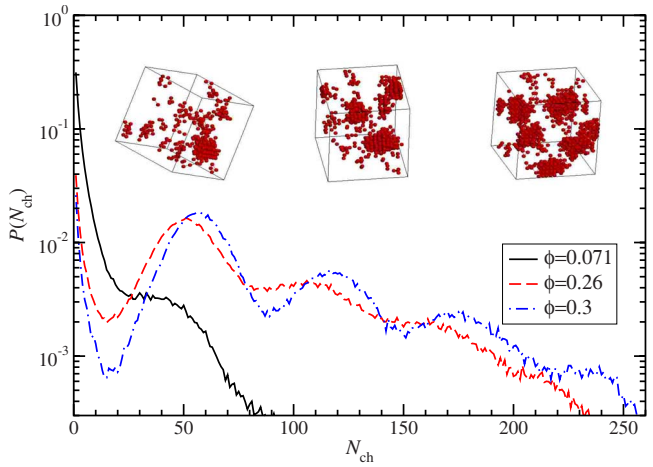

FIG. 2. (Color online) Probability density $P(N_{ch})$ for finding clusters that contain N_{ch} chains, and for different overall monomer concentrations ϕ, indicated in the legend. The histograms are for an $H(H_6T_4)_3$ system at $T^*=4.4$. The insets show simulation snapshots of the end monomers at the quoted values of the concentration ϕ, increasing from left to right.

tion results in the formation of new micelles and only slightly in the growth of the existing ones. At the same time, the $P(N_{ch})$ curves reveal an intriguing feature, namely, the appearance of cluster maxima at aggregation numbers $g_k = kg_0$, $k=2,3,\ldots$, that are integer multiples of the fundamental micellar size g_0. These maxima do not describe spherical micelles of multiple size of the fundamental ones but rather superclusters of g_0-aggregated micelles that are connected through dangling telechelic chains from TSP's that are outside the micellar core. This is, evidently, a peculiar property of the star architecture; it is not present for the case of diblock copolymers [7]. The "higher harmonics" g_k are limited to $k=2$ for the less attractive system, $H(H_8T_2)_3$, Fig. 3, but superaggregates of up to $k=4$ can be seen in the histograms for $H(H_6T_4)_3$ in Fig. 2. TSP's offer thus the possibility of a novel form of supramolecular aggregation through the formation of self-organized micelles that are further connected by threads of individually associating telechelic

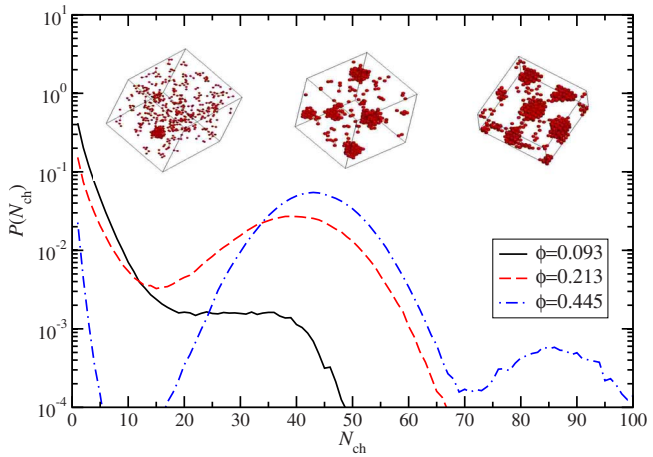

FIG. 3. (Color online) Same as Fig. 2 but for an $H(H_8T_2)_3$ system at temperature $T^*=2.3$.

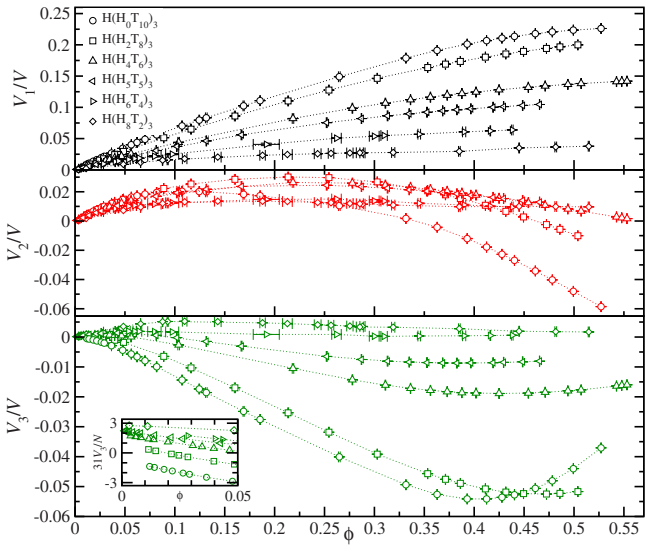

FIG. 4. (Color online) Minkowski functionals V_i, $i=1,2,3$, of the patterns formed by terminal monomers (see the text). From top to bottom: surface area $V_1(\phi)$, mean curvature $V_2(\phi)$, and Euler characteristic $V_3(\phi)$, all per unit volume. The values of T^* are: 15.25$[H(H_0T_{10})_3]$; 10.25$[H(H_2T_8)_3]$; 6.9$[H(H_4T_6)_3]$; 5.8$[H(H_5T_5)_3]$; 4.4$[H(H_6T_4)_3]$; and 2.3$[H(H_8T_2)_3]$. The inset in the bottom panel shows V_3 per TSP.

chains. In this way, micellar oligomers are formed in a polydisperse solution, coexisting with isolated TSP's as well as unconnected micelles.

Quantitative information into the self-assembly of the terminal monomers can be gained by the $d+1$ Minkowski functionals $\mathcal{V}_i$, $i=0,1,\ldots,d$, that form a complete class of additive morphological measures for characterizing size, shape and connectivity of spatial patterns in d dimensions [31–33]. In this approach, every site occupied by a terminal monomer is denoted as "full" and all others as "empty." $\mathcal{V}_0$ is trivial and equal to the number of occupied sites, $\mathcal{V}_1$ is the total exposed surface area between full and empty sites, $\mathcal{V}_2$ is the integral mean curvature, and $\mathcal{V}_3$ is the Euler characteristic, a topological invariant describing connectivity. For the latter, it holds that $\mathcal{V}_3=\mathcal{N}_D+\mathcal{N}_C-\mathcal{N}_T$, where $\mathcal{N}_D$ is the number of disconnected components, $\mathcal{N}_C$ is the number of cavities, and $\mathcal{N}_T$ is the number of tunnels. Thus, spatial structures with a bicontinuous texture result into $\mathcal{V}_3<0$.

Results for the quantities $V_i \equiv \langle \mathcal{V}_i \rangle_{\mu,V,T}$ per volume are shown in Fig. 4 as functions of ϕ for all systems studied. For the phase-separating systems, we choose temperatures that are slightly supercritical for each system, to provide a fair comparison. The exposed surface area V_1 (Fig. 4 upper panel) increases monotonically with ϕ and the number of sticky groups per molecule. Indeed, for small values of λ, formation of spherical micelles results into a reduction of the exposed area, since a sphere has the minimum area for a given volume and the terminal monomers are densely packed in its core. The integral mean curvature V_2 (Fig. 4 middle panel) remains positive for most systems and monomer concentrations; this is consistent with micelle formation for the $\lambda<1/2$ cases. However, for the two most attractive systems, $\lambda=1$ and $8/10$, regions of $V_2<0$ can be discerned at high

concentrations, pointing to the formation of structures in which one of the principal radii of curvature is negative, as occurs in bicontinuous phases. The assertion of formation of such structures is further supported by the Euler characteristic V_3 (Fig. 4, lower panel). Here, it can be seen that all phase-separating systems feature broad regions of tunnel phases, evidenced by $V_3<0$, with both the ϕ range of such occurrences and the magnitude of V_3 growing with λ. For micelle-forming systems, the Euler characteristic remains small and positive. It first grows with ϕ and subsequently it slightly decreases and saturates to a higher value for the less attractive system than for the one with more stickers. This is understood as arising from the intermicellar connections, which reduce the number $\mathcal{N}_D$ of disconnected components, without creating new tunnels; for the systems at hand, $\mathcal{N}_C$ practically vanishes, since there are no hollow micelle cores. As there are fewer intermicellar connections for $\lambda=2/10$ than for $\lambda=4/10$, $\mathcal{N}_D$ for the former is larger, resulting in a higher value of V_3. Finally, in the inset of the lower panel of Fig. 4, we show V_3 per TSP in the low-ϕ region, where the shapes are dominated by intramolecular association. In the absence of the latter, $(3n+1)V_3/N \to f=3$ as $\phi \to 0$, as is indeed the case for the least attractive system, $H(H_8T_2)_3$. However, for a higher number of stickers, the limiting value is smaller, offering evidence of intramolecular association [22].

We have analyzed the aggregation behavior of trifunctional, telechelic star polymers with a variable number of stickers. Our findings are relevant for the control of the rheology of such systems, as the latter is intricately related to the connectivity of the resulting spatial arrangements. Future work should be directed toward the study of TSP's in which not all arms are functionalized and to the effects of changing the functionality f, the monomers n per chain and the rigidity of the latter [34]. Finally, it would be interesting to examine the adsorption of TSP's on suitably treated rigid or fluctuating surfaces.

We thank F. Sciortino and D. Vlassopoulos for a critical reading of the manuscript. F.L.V. has been supported by the Foundation Blanceflor Boncompagni-Ludovisi, née Bildt, and thanks M. Della Morte for helpful discussions, J. Davis for technical support, and the Erwin Schrödinger Institute (ESI, Vienna) for its hospitality. A.Z.P. acknowledges support from the Princeton Center for Complex Materials, and C.N.L. acknowledges Princeton University and the ESI for their hospitality.

[1] S. C. Glotzer and M. J. Solomon, Nature Mater. **6**, 557 (2007).
[2] E. Bianchi, J. Largo, P. Tartaglia, E. Zaccarelli, and F. Sciortino, Phys. Rev. Lett. **97**, 168301 (2006).
[3] D. Nykypanchuk *et al.*, Nature (London) **451**, 549 (2008).
[4] S. Y. Park *et al.*, Nature (London) **451**, 553 (2008).
[5] C. W. Hsu *et al.*, Proc. Natl. Acad. Sci. U.S.A. **105**, 13711 (2008).
[6] A. Z. Panagiotopoulos *et al.*, Langmuir **18**, 2940 (2002).
[7] C. Pierleoni, C. Addison, J. P. Hansen, V. Krakoviack, Phys. Rev. Lett. **96**, 128302 (2006).
[8] B. Capone *et al.*, J. Phys. Chem. B (to be published).
[9] F. Lo Verso and C. N. Likos, Polymer **49**, 1425 (2008).
[10] S. R. Bhatia and W. B. Russel, Macromolecules **33**, 5713 (2000).
[11] P. I. Hurtado, L. Berthier, and W. Kob, Phys. Rev. Lett. **98**, 135503 (2007).
[12] E. Eiser, J. Klein, T. A. Witten, and L. J. Fetters, Phys. Rev. Lett. **82**, 5076 (1999).
[13] J. Klein, J. Phys.: Condens. Matter **12**, A19 (2000).
[14] M. Björling, Macromolecules **31**, 9026 (1998).
[15] A. G. Zilman and S. A. Safran, Eur. Phys. J. E **4**, 467 (2001).
[16] X.-X. Meng and W. B. Russel, Macromolecules **36**, 10112 (2003).
[17] M. Pitsikalis *et al.*, Macromolecules **29**, 179 (1996).
[18] D. Vlassopoulos *et al.*, J. Chem. Phys. **111**, 1760 (1999).
[19] D. Vlassopoulos *et al.*, Macromolecules **33**, 9740 (2000).
[20] F. Ganazzoli *et al.*, Macromol. Theory Simul. **10**, 325 (2001).
[21] R. Connolly *et al.*, J. Chem. Phys. **119**, 8736 (2003).
[22] F. Lo Verso, C. N. Likos, C. Mayer, and H. Lowen, Phys. Rev. Lett. **96**, 187802 (2006); J. Phys. Chem. C **111**, 15803 (2007).
[23] A. Z. Panagiotopoulos *et al.*, Macromolecules **31**, 912 (1998).
[24] M. A. Floriano *et al.*, Macromolecules **38**, 2475 (2005).
[25] R. G. Larson *et al.*, J. Chem. Phys. **83**, 2411 (1985).
[26] D. Frenkel and B. Smit, *Understanding Molecular Simulation* (Academic Press, London, 1996).
[27] A. M. Ferrenberg and R. H. Swendsen, Phys. Rev. Lett. **61**, 2635 (1988); **63**, 1195 (1989).
[28] A. Z. Panagiotopoulos, J. Phys.: Condens. Matter **12**, R25 (2000).
[29] A. D. Bruce and N. B. Wilding, Phys. Rev. Lett. **68**, 193 (1992).
[30] M. Müller and N. B. Wilding, Phys. Rev. E **51**, 2079 (1995).
[31] L. A. Santaló, *Integral Geometry and Geometric Probability* (Addison-Wesley, Reading, MA, 1976).
[32] C. N. Likos *et al.*, J. Chem. Phys. **102**, 9350 (1995).
[33] N. Hoffmann, F. Ebert, C. N. Likos, H. Lowen, and G. Maret, Phys. Rev. Lett. **97**, 078301 (2006); N. Hoffmann, C. N. Likos, and H. Lowen, J. Phys.: Condens. Matter **18**, 10193 (2006).
[34] V. Firetto *et al.*, Langmuir **22**, 6514 (2006).